Notes

Contribution from the Departments of Chemistry,
The University of North Carolina at Charlotte,
Charlotte, North Carolina 28223,
The University of North Carolina,
Chapel Hill, North Carolina 27514,
and North Carolina State University,
Raleigh, North Carolina 27650

A Novel Copper(II) Complex Containing the Ligand 1,2-Bis(2,2′-bipyridyl-6-yl)ethane: Structural, Magnetic, Redox, and Spectral Properties

Ty Garber,† Shawn Van Wallendael,† D. Paul Rillema,*,† Martin Kirk,‡ William E. Hatfield,‡ Jane H. Welch,§ and P. Singh§

Received September 25, 1989

Introduction

Recently our research has involved studies related to documenting the physical and photophysical properties of macrocyclic ligand complexes of nickel(II), cobalt(II), and copper(II)[1-3] and studies on the properties and photophysical characteristics of heterocyclic ligand complexes of ruthenium(II), platinum(II), and rhenium(I).[4-6] In this study, we have amalgamated portions of the two by preparing an open-ended tetradentate ligand based on 2,2′-bipyridine and coordinating the ligand to copper(II). Our ultimate goal is to fabricate closed-ended macrocyclic ligands based on 2,2′-bipyridine, which may behave as porphyrin analogues.

There is good precedence for starting with the open-ended tetradentate ligand. Considerable investigations of copper bis(heterocyclic ligand) complexes have been reported and were summarized by Hathaway and Billing.[7] Past papers generally reported solid-state properties of the complexes due to the fact that the complexes are labile in solution. This is in contrast to copper(II) macrocyclic ligand systems where the axial positions are labile but the remainder of the molecule remains intact. The copper(II) complex containing the open-ended tetradentate ligand would be expected to have properties intermediate in behavior between the two extremes.

In this paper, we report the synthesis of the tetradentate ligand, 1,2-bis(2,2′-bipyridyl-6-yl)ethane, shown in Figure 1, the synthesis of its copper(II) and copper(I) complexes, the X-ray structure of the copper(II) complex and the solid-state and solution properties of the complexes. The properties are interpreted on the basis of existing theories and compared to the properties of other copper(II) heterocycles containing the ligands shown in Figure 1.

Experimental Section

Materials. Cupric acetate monohydrate and 2,2′-bipyridine were purchased commercially and used without further purification. Tetrahydrofuran (THF) was dried and collected over sodium benzophenone ketyl. All other solvents were purchased commercially as HPLC grade and used without further purification. Lithium diisopropylamide and methylithium solutions were provided by Lithco and their weight percentages were determined by NMR integration.[8] Tetrabutylammonium hexafluorophosphate (TBAH) was purchased commercially as electrometric grade and used without further purification. Elemental analyses were performed by Atlantic Microlabs, Inc., Norcross, GA.

Preparation of Compounds. 6-Methyl-2,2′-bipyridine. The preparation followed the procedures of Kauffmann et al.[9] A 45 mL solution of 1.5 M methyllithium in THF (67.5 mmol) was added dropwise to 400 mL of a diethyl ether solution containing 10.62 g (68.0 mmol) of 2,2′-bipyridine at 0 °C. After addition was complete (approximately 2 h), the resulting maroon solution was gently refluxed for 3 h under N_2. It was then allowed to cool to room temperature. A 50-mL portion of water was added with stirring, resulting in a biphasic yellow solution. The aqueous layer was separated from the organic layer and extracted three times with ether. The washings were combined with the organic layer, and the resulting solution was dried by washing twice with brine followed by addition of anhydrous Na_2SO_4 to remove residual water. The solution was then decanted into a round-bottom flask and the ether was removed by rotary evaporation. The resulting orange oil was oxidized with approximately 600 mL of a saturated $KMnO_4$/acetone solution until formation of MnO_2 ceased. The MnO_2 was removed by vacuum filtration through Celite. The filtrate was placed in a round-bottom flask and acetone was removed by rotary evaporation. The dark oil that resulted was distilled at 4.5 mmHg, collecting 8.33 g (72% yield) of light yellow oil at 107–110 °C. ^{1}H NMR: singlet (3 H), 2.61 ppm; doublet (1 H), 7.13 ppm; split triplet (1 H), 7.25 ppm; triplet (1 H), 7.67 ppm; split triplet (1 H), 7.77 ppm; doublet (1 H), 8.13 ppm; doublet (1 H), 8.38 ppm; doublet (1 H), 8.65 ppm.

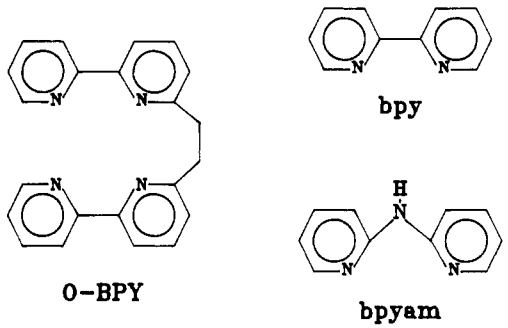

Figure 1. Ligands: O-BPY = 1,2-bis(2,2′-bipyridyl-6-yl)ethane, bpy = 2,2′-bipyridine, bpyam = bis(2-pyridyl)amine.

1,2-Bis(2,2′-bipyridyl-6-yl)ethane. The procedures used were modifications of those used to prepare the -4-yl analogue.[10] A solution consisting of 23.8 mL of 2.0 M (47.6 mmol) lithium diisopropylamide (in hexanes) and 100 mL of dry THF was prepared under N_2. This solution was chilled to −95 °C in a methanol/liquid N_2 bath. After chilling, 8.10 g of 6-methyl-2,2′-bipyridine (47.65 mmol) dissolved in 75 mL of dry THF was added over a 2-h period. The solution was allowed to stir for an additional hour before the addition of 8.2 mL (95.2 mmol) of 1,2-dibromoethane. The resulting solution was allowed to warm to −30 °C and then 50 mL of water was added, resulting in formation of white precipitate in a yellow supernatent. The precipitate was removed by

(1) Bailey, C. L.; Bereman, R. D.; Rillema, D. P. *Inorg. Chem.* **1984**, *23*, 3956. Rillema, D. P.; Bailey, C. L.; Bereman, R. D.; Nowak, R. *Inorg. Chem.* **1986**, *25*, 933. Bailey, C. L.; Bereman, R. D.; Rillema, D. P. *Inorg. Chem.* **1986**, *25*, 3149. Bailey, C. L.; Bereman, R. D.; Rillema, D. P.; Nowak, R. *Inorg. Chim. Acta* **1986**, *116*, L45.
(2) Harrison, J. R.; Rillema, D. P.; Sando, J. J.; Ham, J. H. *Cancer Res.* **1986**, *46*, 5571.
(3) Granifo, J.; Rillema, D. P.; Ferraudi, G. *J. Photochem.* **1983**, *23*, 51. Ferraudi, G.; Rillema, D. P.; Ham, J. H.; Barrera, P.; Granifo, J. *Inorg. Chem.* **1985**, *24*, 281. Geiger, D. K.; Ferraudi, G.; Madden, K.; Granifo, J.; Rillema, D. P. *J. Phys. Chem.* **1985**, *89*, 3890.
(4) Allen, G.; Rillema, D. P.; Meyer, T. J.; White, R. P. *J. Am. Chem. Soc.* **1984**, *106*, 2613. Sahai, R.; Morgan, L.; Rillema, D. P. *Inorg. Chem.* **1988**, *27*, 3495. Ross, H. B.; Boldaji, M.; Blanton, C. B.; Rillema, D. P.; White, R. P. *Inorg. Chem.* **1989**, *28*, 1013.
(5) Sahai, R.; Baucom, D. A.; Rillema, D. P. *Inorg. Chem.* **1986**, *25*, 3843. Sahai, R.; Rillema, D. P. *J. Chem. Soc., Chem. Commun.* **1986**, 1133.
(6) Sahai, R.; Rillema, D. P.; Shaver, R. J.; Van Wallendael, S.; Jackman, D. C. *Inorg. Chem.* **1989**, *28*, 1022. Winslow, L. N.; Rillema, D. P.; Welch, J. H.; Singh, P. *Inorg. Chem.* **1989**, *28*, 1596.
(7) Hathaway, B. J.; Billing, D. E. *Helv. Chim. Acta* **1970**, *5*, 143.
(8) Hatch, Helen B., Lithco. Private communication.
(9) Kauffmann, T.; Konig, J.; Woltermann, A. *Chem. Ber.* **1976**, *109*, 3864.
(10) Elliott, C. M.; Freitag, R. A. *J. Chem. Soc., Chem. Commun.* **1985**, 156. Elliott, E. M.; Freitag, R. A.; Blaney, D. D. *J. Am. Chem. Soc.* **1985**, *107*, 4647.

† The University of North Carolina at Charlotte.
‡ The University of North Carolina.
§ North Carolina State University.

0020-1669/90/1329-2863$02.50/0

Table I. Crystallographic Data for $[Cu(O\text{-}BPY)](ClO_4)_2$

$CuC_{22}H_{18}N_4Cl_2O_8$	space group = $C2/c$
fw = 600.85	T = 298 K
a = 17.966 (4) Å	λ = 0.71069 Å
b = 10.702 (4) Å	d_{calc} = 1.70 g/cm^3
c = 15.527 (4) Å	μ = 12.6 cm^{-1}
β = 128.36 (2)°	$R(F_o)$ = 0.042
V = 2341 (1) Å^3	$R_w(F_o)$ = 0.056
Z = 4	

vacuum filtration, and the THF was removed by rotary evaporation, yielding an additional amount of white precipitate. The precipitate was dissolved in hot methanol, allowing recrystallization of 10.3 g (60%) of white needles, mp 151–153 °C. ^{1}H NMR: singlet (4 H), 3.43 ppm; doublet (2 H), 7.17 ppm; multiplet (2 H), 7.29 ppm; triplet (2 H), 7.69 ppm; twinned triplet (2 H), 7.80 ppm; doublet (2 H), 8.67 ppm; Anal. Calcd for $C_{22}H_{18}N_4$: C, 78.1; H, 5.4; N, 16.6. Found: C, 78.2; H, 5.5; N, 16.5.

$[Cu(O\text{-}BPY)](ClO_4)_2$ (O-BPY = 1,2-Bis(2,2′-bipyridyl-6-yl)ethane). A solution containing 0.11 g (0.53 mmol) of cupric acetate monohydrate dissolved in 30 mL of warm methanol was added dropwise over a 15-min period to a stirring solution containing 0.18 g (0.53 mmol) of free ligand dissolved in 30 mL of warm methanol. A dark green solution resulted, which was allowed to stir for an additional 30 min. About 12 drops of saturated aqueous $NaClO_4$ was added to precipitate the complex as the perchlorate salt. The medium blue precipitate was isolated by vacuum filtration. It was washed with cold ethanol and diethyl ether. The yield was 0.28 g (72%). A suitable crystal for X-ray diffraction analysis was grown by slow evaporation from a 4:1 acetonitrile–toluene solution. Anal. Calcd for $CuC_{22}H_{18}N_4O_8Cl_2$: C, 43.98; H, 3.02; N, 9.32; Cl, 11.80. Found: C, 44.07; H, 3.05; N, 9.30; Cl, 11.73. *Caution!* Perchlorate salts are potentially explosive!

$[Cu(O\text{-}BPY)](ClO_4)$. A solution containing 0.088 g (0.50 mmol) L-(−)-ascorbic acid dissolved in approximately 30 mL of warm absolute methanol was added dropwise to a stirring solution containing 0.152 g (0.25 mmol) of $[Cu(O\text{-}BPY)](ClO_4)_2$ in 20 mL of acetonitrile. During the addition, the color of the solution changed from green to brick red. The solution was allowed to stir for an addition $^1/_2$ h, and the resulting copper(I) perchlorate salt was precipitated by addition of ether. The precipitate was isolated by vacuum filtration, redissolved in acetonitrile, and reprecipitated by addition of ethyl ether. The compound was collected by vacuum filtration and dried under vacuum. The yield was 0.108 g (71%). Anal. Calcd for $CuC_{22}H_{18}N_4O_4Cl$: C, 52.7; H, 3.62; N, 11.17; Cl, 7.07. Found: C, 52.9; H, 3.63; N, 11.12; Cl, 7.04. *Caution!* Perchlorate salts are potentially explosive!

Physical Measurements. Visible–UV spectra were recorded with Perkin-Elmer Lambda Array 3840 and Cary 14 spectrophotometers. The Cary 14 was modified with a R928 phototube and quartz–halogen lamp to extend its range beyond the visible region to approximately 950 nm. Cyclic voltammograms were obtained in various solvents containing 0.10 M TBAH as the supporting electrolyte. The measurements were made vs a Ag/AgCl (nominally −0.044 V vs SSCE) and/or a saturated sodium calomel electrode (SSCE). Electrochemistry was carried out with a PAR 173 potentiostat in conjunction with a PAR 175 programmer. Cyclic voltammograms were recorded with a YEW 3022-A4 X-Y recorder. NMR spectra were recorded in deuterated chloroform with a 300-MHz General Electric QE-300 NMR spectrometer. EPR spectra were recorded with an X-band JEOL Model JES-PE spectrometer and calibrated with DPPH (g = 2.0037). Magnetic susceptibility measurements of finely ground powdered samples contained in Lucite sample holders were measured to 1.0 T by using a Princeton Applied Research Model 155 Foner-type[11] vibrating-sample magnetometer as described previously.[12] The magnetometer was calibrated with $HgCo(NCS)_4$,[13] and the experimental magnetic susceptibility data were corrected for the diamagnetism of constituent atoms by Pascal's constants.[14]

Collection and Reduction of X-ray Data. X-ray data were collected on a Nicolet R3 m/μ diffractometer using the θ–2θ method. A total of 2368 reflections were recorded to a 2θ value of 50°. Data were corrected for Lorentz and polarization effects. Atomic scattering factors for all atoms were obtained from ref 15. The copper and chlorine atoms were located by direct methods and the remaining non-hydrogen atoms were found by conventional difference Fourier techniques to give a trial structure. The structure was refined by the block-diagonal least-squares technique using SHELXTL[16] on the Data General Microeclipse computer. The non-hydrogen atoms were refined with anisotropic temperature factors. The hydrogen atoms were placed 0.96 Å away from attached carbon atoms and were not refined. The single-crystal X-ray crystallographic analysis data are given in Table I.

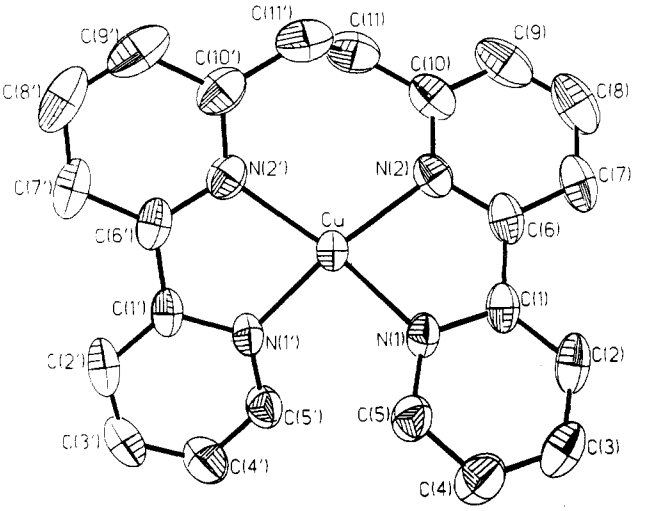

Figure 2. ORTEP diagram of the $[Cu(O\text{-}BPY)]^{2+}$ cation.

Scheme I. Synthesis of 1,2-Bis(2,2′-bipyridyl-6-yl)ethane

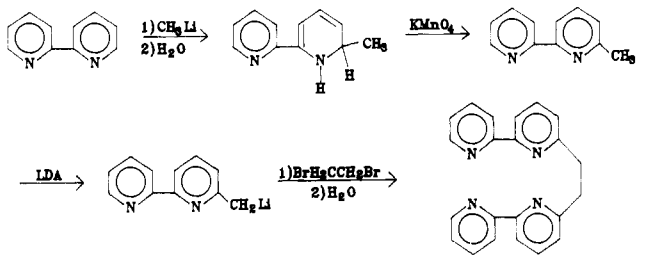

Results

Ligand Synthesis. The tetradentate ligand was synthesized as outlined in Scheme I. The procedure was analogous to the one published by Elliott and co-workers[10] for the analogue with the bridge in the 4- (or 4′-) position. Methylation of 2,2′-bipyridine (bpy) in the 6-position was achieved by reacting bpy with methyllithium at 0 °C, quenching with water, and then oxidizing the reduced intermediate with $KMnO_4$. The resulting 6-methyl-2,2′-bipyridine was then metalated with lithium diisopropylamide at low temperature and coupled by use of 1,2-dibromoethane, which acts as an electron-transfer agent in the coupling process. The temperature at which the coupling was carried out was crucial for obtaining acceptable yields. At −95 °C, a 60% yield was obtained whereas at −77 °C only an 11% yield was achieved.

Preparation and Structure. The copper(II) complex was readily prepared by the addition of copper(II) acetate to a methanol solution of the ligand, O-BPY, and precipitated as the perchlorate salt upon the addition of a solution of sodium perchlorate. The complex was reduced to its copper(I) analogue upon addition of ascorbic acid to an acetonitrile solution of the copper(II) complex. A suitable crystal for X-ray diffraction analysis was isolated from a 4:1 acetonitrile–toluene solution.

The single-crystal X-ray crystallographic analysis positional parameters are given in Table II. Figure 2 shows an ORTEP

(11) Foner, S. *Rev. Sci. Instrum.* **1959**, *30*, 548.
(12) Crovan, P. J.; Estes, W. E.; Weller, R.; Hatfield, W. E. *Inorg. Chem.* **1980**, *19*, 1297.
(13) Brown, D. B.; Crawford, V. H.; Hall, J. W.; Hatfield, W. E. *J. Phys. Chem.* **1977**, *81*, 1303 and references therein.
(14) (a) Figgis, B. N.; Lewis, J. In *Modern Coordination Chemistry*; Lewis, J., Wilkins, R. G., Eds.; Interscience: New York, 1960; Chapter 6, p 403. (b) Konig, E. *Magnetic Properties of Transition Metal Compounds*; Springer-Verlag: West Berlin, 1966. (c) Weller, R. R.; Hatfield, W. E. *J. Chem. Educ.* **1980**, *19*, 1095.
(15) *International Tables for X-ray Crystallography*; Kynoch Press: Birmingham, England, 1974; Vol. IV, pp 71–102.
(16) SHELXTL. X-ray Instruments Group, Nicolet Instrument Corp., Madison, WI.

Table II. Atomic Coordinates ($\times 10^4$) and Isotropic Thermal Parameters ($Å^2 \times 10^3$)

	x	y	z	U[a]
Cu	5000	81 (1)	2500	41 (1)
N(1)	4891 (2)	1322 (3)	3372 (2)	41 (2)
C(1)	4326 (3)	959 (4)	3627 (3)	43 (2)
C(2)	4109 (3)	1772 (5)	4134 (3)	57 (3)
C(3)	4487 (3)	2953 (4)	4400 (4)	63 (3)
C(4)	5094 (3)	3301 (5)	4178 (4)	63 (3)
C(5)	5285 (3)	2461 (4)	3679 (3)	48 (2)
N(2)	4326 (2)	-1008 (3)	2885 (2)	43 (2)
C(6)	3995 (3)	-348 (4)	3331 (3)	47 (2)
C(7)	3394 (3)	-866 (5)	3504 (4)	61 (3)
C(8)	3125 (4)	-2101 (5)	3216 (4)	76 (3)
C(9)	3462 (3)	-2758 (5)	2771 (4)	72 (3)
C(10)	4068 (3)	-2216 (4)	2605 (3)	53 (2)
C(11)	4455 (3)	-2917 (4)	2131 (4)	62 (3)
Cl	2505 (1)	120 (1)	227 (1)	46 (1)
O(1)	2934 (3)	1111 (4)	1003 (3)	101 (3)
O(2)	1902 (2)	601 (3)	-866 (3)	67 (2)
O(3)	1993 (3)	-616 (5)	430 (3)	109 (3)
O(4)	3272 (3)	-552 (4)	401 (3)	100 (3)

[a] Equivalent isotropic U is defined as one-third of the trace of the orthogonalized U_{ij} tensor.

Table III. Bond Distances (Å) and Angles (deg)

Bond Distances			
Cu-N(1)	1.990 (4)	Cu-N(2)	2.021 (4)
Cu-N(1′)	1.990 (4)	Cu-N(2′)	2.021 (4)
N(1)-C(1)	1.355 (7)	N(1)-C(5)	1.340 (5)
C(1)-C(2)	1.382 (8)	C(1)-C(6)	1.478 (6)
C(2)-C(3)	1.372 (7)	C(3)-C(4)	1.382 (10)
C(4)-C(5)	1.364 (8)	N(2)-C(6)	1.358 (7)
N(2)-C(10)	1.351 (5)	C(6)-C(7)	1.380 (9)
C(7)-C(8)	1.382 (8)	C(8)-C(9)	1.363 (10)
C(9)-C(10)	1.392 (9)	C(10)-C(11)	1.490 (9)
C(11)-C(11′)	1.538 (9)	Cl-O(1)	1.422 (4)
Cl-O(2)	1.427 (3)	Cl-O(3)	1.388 (6)
Cl-O(4)	1.423 (6)		
Bond Angles			
N(1)-Cu-N(2)	81.6 (2)	N(1)-Cu-N(1′)	96.4 (2)
N(2)-Cu-N(1′)	156.4 (1)	N(1)-Cu-N(2′)	156.4 (1)
N(2)-Cu-N(2′)	109.5 (2)	N(1′)-Cu-N(2′)	81.6 (2)
Cu-N(1)-C(1)	114.6 (3)	Cu-N(1)-C(5)	126.6 (4)
C(1)-N(1)-C(5)	118.8 (4)	N(1)-C(1)-C(2)	121.0 (4)
N(1)-C(1)-C(6)	114.2 (4)	C(2)-C(1)-C(6)	124.8 (5)
C(1)-C(2)-C(3)	119.2 (6)	C(2)-C(3)-C(4)	119.6 (6)
C(3)-C(4)-C(5)	118.7 (5)	N(1)-C(5)-C(4)	122.6 (6)
Cu-N(2)-C(6)	112.6 (3)	Cu-N(2)-C(10)	127.3 (4)
C(6)-N(2)-C(10)	119.4 (5)	C(1)-C(6)-N(2)	115.5 (5)
C(1)-C(6)-C(7)	122.2 (5)	N(2)-C(6)-C(7)	122.2 (4)
C(6)-C(7)-C(8)	118.7 (6)	C(7)-C(8)-C(9)	118.8 (6)
C(8)-C(9)-C(10)	121.6 (5)	N(2)-C(10)-C(9)	119.4 (5)
N(2)-C(10)-C(11)	118.0 (5)	C(9)-C(10)-C(11)	122.7 (4)
C(10)-C(11)-C(11′)	113.7 (4)	O(1)-Cl-O(2)	110.6 (2)
O(1)-Cl-O(3)	108.5 (3)	O(2)-Cl-O(3)	110.7 (2)
O(1)-Cl-O(4)	105.4 (3)	O(2)-Cl-O(4)	109.9 (3)
O(3)-Cl-O(4)	111.7 (3)		

drawing of the cation, and Table III contains bond distances and angles. The two bipyridine rings are related to each other by a C_2 symmetry operation. Consequently, bond lengths for analogous atoms contained in both halves of the molecule are the same. Thus, the Cu-N(2) and Cu-N(2′) bond distances are 2.02 Å and the Cu-N(1) and Cu-N(1′) distances are 1.99 Å. The longer Cu-N(2)(N(2′)) bond distances can be attributed to the presence of the ethyl bridge. The interatomic distance of Cu to the closest oxygen of perchlorate ion is 2.86 Å. If a mean plane is drawn through the copper center and midway between the four nitrogen atom donors, then N(1) would lie 0.42 Å above the plane, N(1′) would lie 0.42 Å below the plane, N(2) would lie 0.37 Å below the plane, and N(2′) would lie 0.37 Å above the plane. The N(2)-Cu-N(2′) bond angle is 109.5°, whereas the N(1)-Cu-N(1′) bond angle is 96.4°. The twist of the pyridine rings about the 2,2′-carbon bonds is 3.5°, and the angle between intramolecular plane normals of the bipyridine rings is 35°.

Table IV. Cyclic Voltammetry Data for the $[Cu(O\text{-}BPY)]^{2+/+}$ Redox Couple in Various Solvents[a]

solvent	$E_{p,red}$, V	$E_{p,ox}$, V	$E_{1/2}$, V	i_c/i_a
acetonitrile	0.20	0.28	0.24	1.0
methylene chloride	0.19	0.26	0.23	0.9
THF	0.17	0.25	0.21	0.9
DMF	0.03	0.50	0.26	1.2
methanol	-0.02	0.46	0.22	1.2
water	-0.16	0.30	0.07	0.3

[a] 0.10 M TBAH, 200 mV/s, error = ±0.02 V.

Table V. Visible-UV Properties of Compounds in Acetonitrile

compound	λ_{max}, nm (ϵ, $cm^{-1}\ M^{-1}$)[a]
$[Cu(O\text{-}BPY)]^{2+}$	620, 685[b]
	714 (1.9×10^2), 363 (3.7×10^2), 308 (1.8×10^4), 243 (1.8×10^4)
$[Cu(O\text{-}BPY)]^{+}$	440 (5.7×10^3), 341 (3.8×10^3), 294 (2.5×10^4), 266 (2.4×10^4), 246 (2.4×10^4)

[a] λ_{max}, ±1 nm; ϵ, ±0.1 $cm^{-1}\ M^{-1}$. [b] Solid state.

Solid-State Properties. Magnetic Susceptibility. The temperature dependent magnetic susceptibility results followed the Curie-Weiss law. The $1/\chi$ vs T plot was linear with a Curie constant of 2.0 ± 0.03 and a Weiss constant of -0.67 ± 0.07 K. The field dependence of the magnetism was also tested and found to be essentially linear to 1 T displaying no sign of saturation. The effective magnetic moment of the complex was 1.90 ± 0.01 μ_B. This value is in the range of 1.8–2.0 μ_B found for other copper(II) complexes in a magnetically dilute environment. The values are higher than the spin only value (1.73 μ_B) due to mixing-in of angular momentum from excited states via spin–orbit coupling.[14a]

Electron Spin Resonance. The ESR spectrum of polycrystalline $[Cu(O\text{-}BPY)](ClO_4)_2$ is shown in Figure 3. The spectrum can best be described as isotropic with a weak $g_\parallel$ component located at 2.21 ± 0.01 and $g_\perp$ located at 2.09 ± 0.01. The spectrum is similar to the one for $[Cu(bpy)_2](PF_6)_2$, except that in the latter case $g_\parallel$ is better resolved.[17]

Visible Spectrum. The visible spectrum of the polycrystalline complex was obtained in a Nujol mull. The experimental envelope shown in Figure 4a was deconvoluted into three transitions by using Gaussian line-shape analysis. The possible dd transitions can best be explained by the angular overlap model, which results in the dd orbital splitting pattern shown in Figure 5.[18] The $d_{x^2-y^2}$ orbital was reported[17] to contain the unpaired electron in $[Cu(bpy)_2](PF_6)_2$, and this is expected to be the case here as well. In addition, single-crystal polarization studies of $[Cu(bpyam)_2](ClO_4)_2$ revealed that the transition energies were in the order $d_{yz} \rightarrow d_{x^2-y^2} > d_{z^2} \rightarrow d_{x^2-y^2} > d_{xy} \rightarrow d_{x^2-y^2}$.[19] Thus, the dd transitions in $[Cu(O\text{-}BPY)]^{2+}$ are assigned as $d_{xz,yz} \rightarrow d_{x^2-y^2}$ (16 440 cm^{-1}), $d_{z^2} \rightarrow d_{x^2-y^2}$ (13 980 cm^{-1}) and $d_{xy} \rightarrow d_{x^2-y^2}$ (12 535 cm^{-1}).

Solution Processes. Electrochemistry. Redox processes were investigated by cyclic voltammetry, and the results are summarized in Table IV. The $[Cu(O\text{-}BPY)]^{2+/+}$ couple behaved near ideality in acetonitrile. The i_c/i_a ratio was nearly one and a plot of the square root of the sweep rate vs ΔE_p, where $\Delta E_p = E_{p,ox} - E_{p,red}$, had an intercept of 76 mV, somewhat larger than the 59 mV expected for a reversible, one-electron transfer.[20] However, larger separations on the order of 70–80 mV for reversible, one-electron couples often are found in nonaqueous solvents.[21]

(17) Foley, J.; Tyagi, S.; Hathaway, B. J. *J. Chem. Soc., Dalton Trans.* **1984**, 1.
(18) Purcell, K. F.; Kotz, J. C. *Inorganic Chemistry*; Saunders: Philadelphia, PA, 1977; pp 543–545.
(19) Dudley, R. J.; Hathaway, B. J.; Hodgson, P. G. *J. Chem. Soc., Dalton Trans.* **1972**, 822.
(20) Nicholson, R. S.; Shain, I. *Anal. Chem.* **1964**, *36*, 705.
(21) Callahan, R. W.; Brown, G. M.; Meyer, T. J. *Inorg. Chem.* **1975**, *14*, 1443.

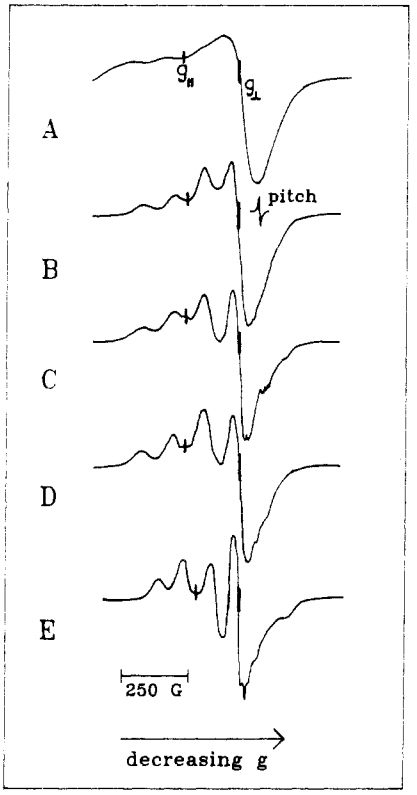

Figure 3. ESR spectra of $[Cu(O\text{-}BPY)](ClO_4)_2$: (A) polycrystalline form; (B) a 20% DMF/80% CH_2Cl_2 glass; (C) a 100% BuCN glass; (D) a 10% DMF/90% BuCN glass; (E) a 10% pyridine/90% BuCN glass. T = 77 K.

In the past, redox potentials for the Cu(II/I) couple of a given copper macrocyclic ligand complex varied with solvent.[22] However, as noted from the data in Table IV, $E_{1/2}$ remained relatively fixed for the $[Cu(O\text{-}BPY)]^{2+/+}$ redox couple in the various solvents examined, except water. Further, the data indicated partial irreversibility ($i_c/i_a > 1$) in methylene chloride and tetrahydrofuran, which become more severe in methanol and dimethylformamide ($i_c/i_a > 1$; $\Delta E_p > 400$ mV).

Visible–UV Spectra. The visible–UV spectra were examined for $[Cu(O\text{-}BPY)]^{2+}$ and $[Cu(O\text{-}BPY)]^{+}$ in acetonitrile, and the data are summarized in Table V. Absorbance for $[Cu(O\text{-}BPY)]^{2+}$ are characterized by low-energy transitions located over the 550–900-nm region and high-intensity transitions in the UV related to intraligand $\pi \rightarrow \pi^*$ transitions. The dd transitions are lost in the d^{10} analogue and replaced by an intermediate-intensity transition located at 440 nm. This intermediate-intensity transition is assigned as a metal to ligand charge-transfer transition (MLCT) by comparison to other copper(I) heterocycles such as $[Cu(2,9\text{-}(CH_3)_2\text{-}1,10\text{-phen})]^{+}$.[22]

The dd absorptions observed in acetonitrile were compared to those observed in other solvents and are illustrated in Figure 4b–e. The spectra are markedly similar consisting of a main absorption maximum and shoulders on both the low-energy and high-energy sides. In pyridine, the low-energy shoulder is much more pronounced than in the other three solvents. Solvent is expected to coordinate in the open coordination sites of $[Cu(O\text{-}BPY)]^{2+}$ resulting in tetragonal complexes. As illustrated in Figure 5, dd absorptions would red-shift from those found in the polycrystalline sample where $[Cu(O\text{-}BPY)]^{2+}$ approaches a square planar geometry. Indeed dd absorption maxima in solution are red-shifted 50 nm or more when compared to the maxima in the polycrystalline sample. Further, the red shift is the greatest for the complex in pyridine, where the bis(pyridine) adduct would most closely model an octahedral complex. The Gaussian deconvolutions of the absorption manifolds illustrate this more clearly. Basically, the same results are obtained in acetonitrile, dimethylformamide, and water. The transitions in pyridine are red-shifted from those found in the other solvents in keeping with the energy level diagram in Figure 5. The data from the deconvolutions tabulated in the Figure 4 legend are in agreement with this assessment.

ESR Spectra. ESR spectra of $[Cu(O\text{-}BPY)]^{2+}$ were obtained in glasses at 77 K and are compared in Figure 3. The spectra are similar and resolved into a parallel and perpendicular component. The values for $g_\perp$ were approximately the same as for the polycrystalline sample ($g_\perp = 2.09$). While $g_\perp$ appears to be the correct designation, single-crystal studies have shown it to be composed of two closely spaced components (g_x and g_y).[7] The $g_\parallel$ values in butyronitrile glasses were 2.33, somewhat higher than the polycrystalline value of 2.20. The 10% py/90% BuCN mixture was an exception to this. The $g_\parallel$ value of $[Cu(O\text{-}BPY)]^{2+}$ in this mixture was 2.28. Within experimental error, $A_\parallel$ was the same for the polycrystalline material and the complex in the butyronitrile glasses. The values were 229×10^{-4} cm^{-1} and 227×10^{-4} cm^{-1}, respectively. Again the 10% py/90% BuCN mixture resulted in an exception. $A_\parallel$ for $[Cu(O\text{-}BPY)]^{2+}$ in this medium was somewhat less, 201×10^{-4} cm^{-1}. The ESR spectral data of the glasses are consistent with a tetragonal model. Published ESR results show tetragonal complexes have $g_\parallel$ values in the 2.2–2.3 range and $g_\perp$ values near 2.05.[7,23]

Discussion

Solid-State Properties. Two structures that can readily be compared to $[Cu(O\text{-}BPY)](ClO_4)_2$ are $[Cu(bpy)_2](PF_6)_2$ and $[Cu(bpyam)_2](ClO_4)_2$. The first compound, $[Cu(bpy)_2](PF_6)_2$, crystallizes in the space group $I4_1/acd$. It has equivalent Cu–N bond lengths of 1.99 Å, a dihedral angle of 46°, equivalent N–Cu–N angles of cis nitrogen atoms on differing bpy units of 104°, and distances of 3.3 Å from copper to the closest fluoride atom of the PF_6^- anions.[17] The second compound, $[Cu(bpyam)_2](ClO_4)_2$, crystallizes in the space group $C2/c$.[19,24] It has two equivalent Cu–N bond lengths of 1.94 and 1.99 Å, a dihedral angle of 56°, equivalent N–Cu–N angles of cis nitrogen atoms on differing bpyam units of 96°, and distances of 3.6 Å from copper to the closest oxygen atom of the ClO_4^- anion. In comparison, $[Cu(O\text{-}BPY)](ClO_4)_2$ crystallizes in the space group $C2/c$. It has two equivalent Cu–N bond distances of 1.99 and 2.02 Å, a dihedral angle of 35°, N–Cu–N angles of cis nitrogen atoms on differing "bpy" units of 96 and 109°, and distances of 2.74 Å from copper to the closest oxygen atom of the ClO_4^- counterion. The complexes fall in the order $[Cu(bpyam)_2]^{2+} > [Cu(bpy)_2]^{2+} > [Cu(O\text{-}BPY)]^{2+}$ based on decreasing dihedral angle. As this angle decreases, one moves closer toward square-planar geometry, and according to Figure 5, the $d_{xz,yz} \rightarrow d_{x^2-y^2}$ transition energy is expected to increase. Thus, this dd transition in $[Cu(O\text{-}BPY)]^{2+}$ would be highest in energy, followed by $[Cu(bpy)_2]^{2+}$ and finally $[Cu(bpyam)_2]^{2+}$. Actually the highest energy absorption for $[Cu(bpyam)_2]^{2+}$ is located at 550 nm,[25] the one for $[Cu(bpy)_2]^{2+}$ is found at 590 nm,[17] and the comparable transition for $[Cu(O\text{-}BPY)]^{2+}$ is located at ~620 nm. There are two possible explanations for this reversal. The first is related to bond-distance changes. In terms of average Cu–N bond lengths, the following trend is observed: $[Cu(bpyam)_2]^{2+} < [Cu(bpy)_2]^{2+} < [Cu(O\text{-}BPY)]^{2+}$. On the basis of the concepts of ligand field theory, the shorter the bonds the greater will be the ligand field strength and hence a greater d orbital splitting. The second possibility is related to the counterion distance from the open axial coordination sites in the three polycrystalline complexes. The counterion in $[Cu(O\text{-}BPY)]^{2+}$ is closest (2.74 Å), followed by $[Cu(bpy)_2]^{2+}$ (3.3 Å) finally $[Cu(bpyam)_2]^{2+}$ (3.6 Å). This ordering is consistent

(22) (a) Ahn, B. T.; McMillin, D. R. *Inorg. Chem.* **1978**, *17*, 2253. (b) McMillin, D. R.; Buckner, M. T.; Ahn, B. T. *Inorg. Chem.* **1977**, *16*, 943.

(23) The values in this paper were calculated at the crossover point as illustrated in Figure 3. Previous reports have used the minimum of the high-field peak. Thus, our values are slightly higher.

(24) Johnson, J. E.; Beineke, T. A.; Jacobson, R. A. *J. Chem. Soc. A* **1971**, 1371.

(25) McWhinnie, W. R. *J. Chem. Soc.* **1964**, 5165.

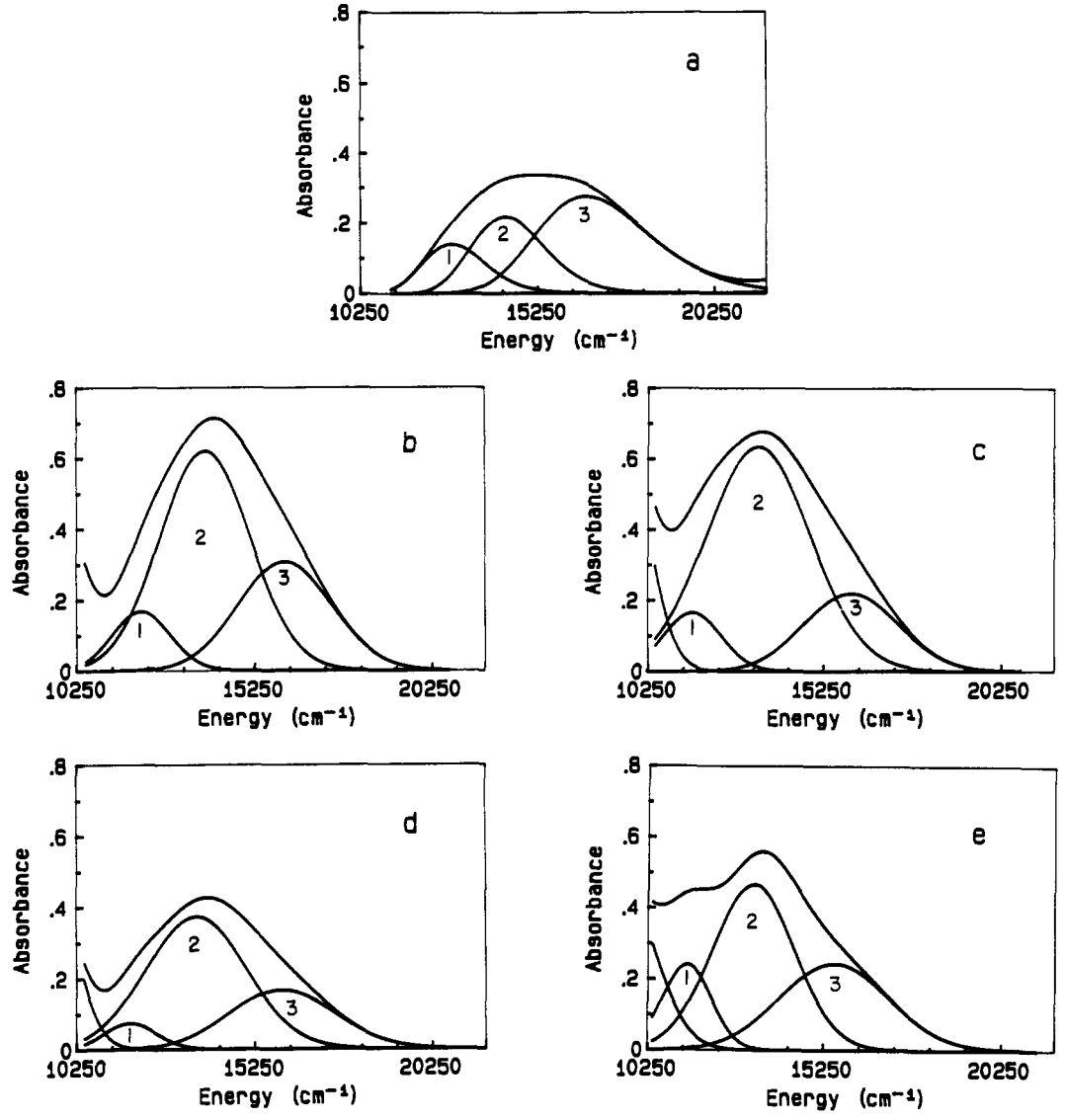

Figure 4. Visible spectrum and Gaussian line-shape analysis of $[Cu(O\text{-}BPY)](ClO_4)_2$ in (a) a Nujol mull (12 535, 13 980, and 16 440 cm^{-1}), (b) acetonitrile (12 050, 13 860, and 16 105 cm^{-1}), (c) DMF (11 640, 13 452, and 16 095 cm^{-1}), (d) H_2O (11 740, 13 600, and 16 000 cm^{-1}), (e) and pyridine (11 345, 13 240, and 15 540 cm^{-1}).

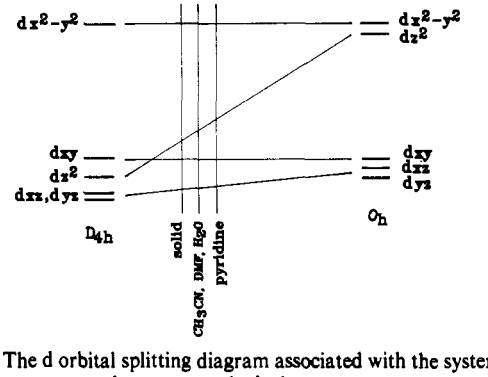

Figure 5. The d orbital splitting diagram associated with the systemmatic change from square planar to octahedral symmetry.

with the observed visible absorptions according to Figure 5. While these distances are longer than what is considered to be normal bond distances, their presence can account for the energy ordering of the dd orbitals in copper(II) "square-planar" complexes.

Solution Properties. $[Cu(O\text{-}BPY)]^{2+}$ exhibits solution properties intermediate in character between those of the bis chelates and those of the macrocyclic ligand complexes. $[Cu(bpy)_2]^{2+}$, for example, undergoes irreversible redox processes in acetonitrile whereas $[Cu(TIM)]^{2+}$, where TIM = 2,3,9,10-Me_4-[14]-1,3,8,10-tetraene-N_4, undergoes a series of reversible oxidations and reductions.[26] The only redox couple observed for $[Cu(O\text{-}BPY)]^{2+}$ is the 2+/1+ process. The $[Cu(O\text{-}BPY)]^{2+/1+}$ couple behaves ideally in acetonitrile, but other complications arise in other solvents. The copper complex of the O-BPY analogue, TET, where TET = 2,2′-bis(2,2′-bipyridyl-6-yl)biphenyl, reportedly has better electrochemical properties, exhibiting both a reversible copper (II/I) couple and reversible bipyridine ligand reductions at negative potentials.[27] The biphenyl bridge distorts the complex toward tetrahedral geometry, which may account for its more electrochemical viability.

The electronic properties of $[Cu(O\text{-}BPY)]^+$ are similar to those of $[Cu(TET)]^+$, $[Cu(bpy)_2]^+$, and $[Cu(dmb)_2]^+$, where dmb is 4,4′-dimethyl-2,2′-bipyridine.[27] The absorbance in the 450-nm region has an absorption coefficient characteristic of MLCT processes and has been assigned as a $d_{xy} \rightarrow \pi^*$ transition.[27] Excitation of $[Cu(2,9\text{-}(CH_3)_2\text{-}1,10\text{-phen})_2]^+$ at this frequency results in emission.[22] $[Cu(O\text{-}BPY)]^+$, however, displays no detectable emission at room temperature or at 77 K.

Acknowledgment. We thank the Office of Basic Energy Sciences, Division of Chemical Sciences, of the Department of Energy under Grant DE-FG05-84ER-13263, the North Carolina Bio-

(26) Maroney, M. J.; Wicholas, M. *Inorg. Chim. Acta* **1983**, *77*, L237.
(27) Muller, E.; Piguet, C.; Berardinelli, G.; Williams, A. F. *Inorg. Chem.* **1988**, *27*, 849.

technology Center, and the National Science Foundation under Grant 88-07498 for support. We also thank Lithco for supplying the organolithium compounds used in the preparations and Randy Shaver for help with the Gaussian analyses.

Supplementary Material Available: Figures showing the Curie–Weiss magnetic susceptibility behavior and the unit cell packing and tables listing X-ray crystal structure parameters, anisotropic thermal parameters, and H atom coordinates and isotropic thermal parameters (6 pages); a table listing observed and calculated structure factors (13 pages). Ordering information is given on any current masthead page.

Contribution from the Research Laboratory of Resources Utilization, Tokyo Institute of Technology, 4259 Nagatsuta, Midori-ku, Yokohama 227, Japan

Preparation and Structure of Mononuclear Iron(III) Complexes $[LFeCl_3]^-$ and $[LFe(N_3)_3]^-$ (L = Hydrotris(1-pyrazolyl)borate and Hydrotris(3,5-dimethyl-1-pyrazolyl)borate)

Hideno Fukui, Masami Ito, Yoshihiko Moro-oka,* and Nobumasa Kitajima*

Received December 27, 1989

The utility of tripod nitrogen ligands $(HB(pz)_3)^-$ and $(HB(3,5\text{-}Me_2pz)_3)^-$ in synthesizing a variety of transition-metal complexes has been demonstrated in recent years.[1] The iron complexes ligated by these ligands are of interest especially from the bioinorganic point of view, because the rigid N_3 ligand coordination mimics the multiimidazole coordination found often in the active site of non-heme iron proteins. The synthesis and characterization of a binuclear iron complex $(HB(pz)_3)FeO(OAc)_2Fe(HB(pz)_3)$ as a synthetic analogue for methemerythrin achieved by Lippard et al.[2] is a good example. However, the marked tendency to form a stable full-sandwich FeL_2 is a serious problem of these ligands. Therefore, to date, a half-sandwich complex $LFeX_n$ is not known, whereas the corresponding iron complex $LFeCl_3$ with a similar tripod nitrogen ligand 1,4,7-triazacyclononane or 1,4,7-trimethyl-1,4,7-triazacyclononane was reported to be a good reactant for syntheses of a series of iron complexes.[3] We now found that the reaction of a binuclear iron(III) complex $(Et_4N)_2(Fe_2OCl_6)$ with $KHB(pz)_3$ or $KHB(3,5\text{-}Me_2pz)_3$ gives the mononuclear iron complex $[LFeCl_3]^-$. The syntheses and structures of the complexes and the azide derivative are described here.

Experimental Section

General Data. Unless otherwise stated, reactions were performed under argon. All reagents were used as received. MeCN was dried over CaH_2 and distilled under an argon atmosphere. $(Et_4N)_2(Fe_2OCl_6)$ (**1**) was prepared by the recently improved synthetic method.[4] $KHB(pz)_3$ and $KHB(3,5\text{-}Me_2pz)_3$ were synthesized by the literature methods.[5] UV–vis and IR spectra were recorded on a Shimazu UV-260 instrument and a Hitachi 250-50 instrument, respectively. Elemental analyses were performed in the service department in the Tokyo Institute of Technology.

Table I. Crystallographic Data for $(Et_4N)[(HB(pz)_3)FeCl_3]$ (**2**) and $(Et_4N)[(HB(3,5\text{-}Me_2pz)_3)Fe(N_3)_3]$ (**4**)

	Compound **2**
$C_{17}H_{30}N_7Fe_1Cl_3B_1$	orthorhombic, *Pcab*
a = 16.993 (3) Å	λ = 0.71068 Å
b = 17.547 (2) Å	μ(Mo Kα) = 9.12 cm^{-1}
c = 16.166 (5) Å	$2° < 2\theta < 60°$
V = 4820 (2) Å^3	no. of measd reflcns = 7963
Z = 8	no. of obsd reflcns ($F_o > 3\sigma(F_o)$) = 2166
fw = 505.5	R = 0.0398
D_{calcd} = 1.40 g cm^{-3}	R_w = 0.0402
	Compound **4**
$C_{23}H_{42}N_{15}Fe_1B_1$	monoclinic, *Cm*
a = 15.443 (5) Å	λ = 0.71068 Å
b = 12.399 (3) Å	μ(Mo Kα) = 4.78 cm^{-1}
c = 10.183 (2) Å	$2° < 2\theta < 60°$
β = 126.37 (1)°	no. of measd reflcns = 2595
V = 1569.8 (7) Å^3	no. of obsd reflcns ($F_o > 3\sigma(F_o)$) = 1975
Z = 2	R = 0.0547
fw = 609.4	R_w = 0.0576
D_{calcd} = 1.29 g cm^{-3}	

$(Et_4N)[(HB(pz)_3)FeCl_3]$ (2). A 0.603-g (1.00-mmol) sample of **1** and 0.448 g (2.00 mmol) of $KHB(pz)_3$ were stirred in 20 mL of MeCN for 20 min. The mixture was filtered over Celite, and the volume of the filtrate was reduced to half under vacuum. Cooling the solution at −20 °C afforded 0.231 g of orange microcrystalline solids (yield 23%). IR (KBr): ν(BH) 2500 cm^{-1}. UV–vis (MeCN): 305 (ϵ = 7600 M^{-1} cm^{-1}), 350 nm (5200). Anal. Calcd for $C_{17}H_{30}N_7BCl_3Fe$: C, 40.39; H, 5.98; N, 19.40; Cl, 21.04. Found: C, 40.40; H, 6.10; N, 19.21; Cl, 21.66.

$(Et_4N)[(HB(3,5\text{-}Me_2pz)_3)FeCl_3]$ (3). A 0.602-g (1.00-mmol) sample of **1** and 0.674 g (2.00 mmol) of $KHB(3,5\text{-}Me_2pz)_3$ were stirred in 20 mL of MeCN for 1 h. The reaction mixture was filtered, and the volume of the brown filtrate was reduced to half under vacuum. Cooling this solution at −20 °C afforded 0.288 g of orange microcrystalline solids (yield 24%). IR (KBr): ν(BH) 2554 cm^{-1}. UV–vis (MeCN): 291 (ϵ = 4800 M^{-1} cm^{-1}), 394 nm (6400). Anal. Calcd for $C_{23}H_{42}N_7BCl_3Fe$: C, 46.85; H, 7.18; N, 16.63; Cl, 18.04. Found: C, 46.80; H, 7.48; N, 16.72; Cl, 18.31.

$(Et_4N)[(HB(3,5\text{-}Me_2pz)_3)Fe(N_3)_3]$ (4). Method A. A 0.602-g (1.00-mmol) sample of **1** and 0.675 g (2.00 mmol) of $KHB(3,5\text{-}Me_2pz)_3$ were stirred in the presence of 0.520 g (8.00 mmol) of NaN_3 in 20 mL of MeCN for 3 h. The reaction mixture was filtered over Celite. The clear reddish brown filtrate was stored at −20 °C to give red microcrystalline solids (0.367 g, yield 30%). IR(KBr): ν(BH) 2541 cm^{-1}; $\nu(N_3)$ 2073, 2048 cm^{-1}. UV–vis (MeCN): 331 (ϵ = 6200 M^{-1} cm^{-1}), 441 (6800), 510 nm (5600). Anal. Calcd for $C_{23}H_{42}N_{16}BFe$: C, 45.34; H, 6.95; N, 36.78. Found: C, 45.30; H, 6.92; N, 36.82.

Method B. A 0.659-g (1.12-mmol) sample of **3** and 0.301 g (4.63 mmol) of NaN_3 were stirred in 30 mL of MeCN for 20 min. The formed precipitate was removed by filtration, and the filtrate was evacuated to dryness to afford **4** as red solids essentially in quantitative yield.

Structure Determinations. Crystals of **2** and **4** suitable for an X-ray analysis were grown from acetone and acetonitrile, respectively. The X-ray data were collected on a Rigaku four-circle diffractometer, Model AFC-5. The lattice parameters were determined by a least-square fit to the automatically centered 25 independent reflections with $2\theta \lesssim 30°$. The crystal parameters and additional details of the data collections are given in Table I. The data were corrected for Lorentz and polarization. Secondary decay was not observed during the data collections for both complexes. The positions of the iron atoms were determined by direct methods. In both cases, the other non-hydrogen atoms were easily located by the subsequent weighted Fourier calculations. The difference Fourier map for **2** showed all of the hydrogen atoms, which were included for the refinements. For **4**, all of the hydrogen atoms except the ones on the cation were found in the difference Fourier map and these were included for the calculations. The structures were refined by full-matrix least-squares methods. The weighting scheme was $w = [\sigma^2(F_o) + (pF_o)^2]^{-1}$ (p = 0.0 for **2** and 0.056 for **4**). The calculations were carried out by CRYSTAN on a FACOM A-70 computer. The final positional parameters for all non-hydrogen atoms of **2** and **4** are listed in Tables II and III, respectively.

Results and Discussion

Despite our expectation at the outset of this work (generation of a novel μ-oxo binuclear complex, $[(HB(pz)_3)FeOFe$-

(1) Trofimenko, S. *Prog. Inorg. Chem.* **1986**, *34*, 115.
(2) (a) Armstrong, W. H.; Lippard, S. J. *J. Am. Chem. Soc.* **1983**, *105*, 4837. (b) Armstrong, W. H.; Spool, A.; Papaefthymiou, G. C.; Frankel, R. B.; Lippard, S. J. *Ibid.* **1984**, *106*, 3653.
(3) (a) Wieghardt, K.; Pohl, K.; Gebert, W. *Angew. Chem., Int. Ed. Engl.* **1983**, *22*, 727. (b) Wieghardt, K.; Pohl, K.; Ventur, D. *Ibid.* **1985**, *24*, 392. (c) Hartman, J. R.; Rardin, R. L.; Chaudhuri, P.; Pohl, K.; Wieghardt, K.; Nuber, B.; Weiss, J.; Papaefthymiou, G. C.; Frankel, R. B.; Lippard, S. J. *J. Am. Chem. Soc.* **1987**, *109*, 7387. (d) Chaudhuri, P.; Winter, M.; Wieghardt, K.; Gehring, S.; Haase, W.; Nuber, B.; Weiss, J. *Inorg. Chem.* **1988**, *27*, 1564. (e) Drueke, S.; Wieghardt, K.; Nuber, B.; Weiss, J. *Ibid.* **1989**, *28*, 1414. (f) Drueke, S.; Wieghardt, K.; Nuber, B.; Weiss, J.; Fleischhauer, H.-P.; Gehring, S.; Haase, W. *J. Am. Chem. Soc.* **1989**, *111*, 8622.
(4) Armstrong, W. H.; Lippard, S. J. *Inorg. Chem.* **1985**, *24*, 981.
(5) Trofimenko, S. *Inorg. Synth.* **1970**, *12*, 99.

0020-1669/90/1329-2868$02.50/0